

Supporting Information

Facile extraction of cellulose nanocrystals from wood using ethanol and peroxide solvothermal pretreatment followed by ultrasonic nanofibrillation

Yanna Li, Yongzhuang Liu, Wenshuai Chen, Qingwen Wang, Yixing Liu, Jian Li, Haipeng Yu*

Key laboratory of Bio-based Material Science and Technology, Ministry of Education, Northeast Forestry University, Harbin 150040, China.

Table S1 Assignment of main ^{13}C - ^1H cross-signals in the HSQC spectra

label	$\delta\text{C}/\delta\text{H}$	assignment
C_β	52.1/3.71	$\text{C}_\beta\text{-H}_\beta$ in phenylcoumarane substructures (C)
B_β	54.0/3.03	$\text{C}_\beta\text{-H}_\beta$ in resinol substructures (B)
$-\text{OCH}_3$	56.1/3.77	C-H in methoxyls
D_β	60.7/3.18	$\text{C}_\beta\text{-H}_\beta$ in spirodienone substructures (D)
A_γ	60.0/3.69 and 60.5/3.83	$\text{C}_\gamma\text{-H}_\gamma$ in $\beta\text{-O-4'}$ substructures (A)
I_γ	62.3/4.22	$\text{C}_\gamma\text{-H}_\gamma$ in <i>p</i> -hydroxycinnamyl alcohol end groups (I)
C_γ	62.8/3.74	$\text{C}_\gamma\text{-H}_\gamma$ in phenylcoumaran substructures (C)
B_γ	71.9/3.79 and 71.9/3.87	$\text{C}_\gamma\text{-H}_\gamma$ in resinol substructures (B)
$(\text{A}, \text{A}')_\alpha$	72.6/4.79	$\text{C}_\alpha\text{-H}_\alpha$ in $\beta\text{-O-4'}$ substructures (A) and γ -acylated $\beta\text{-O-4'}$ substructures (A')
B_α	85.7/4.64	$\text{C}_\alpha\text{-H}_\alpha$ in resinol substructures (B)
$\text{S}_{2,6}$	103.8/6.64	$\text{C}_{2,6}\text{-H}_{2,6}$ in etherified syringyl units (S)
$\text{S}'_{2,6}$	106.7/7.34	$\text{C}_{2,6}\text{-H}_{2,6}$ in oxidized ($\text{C}_\alpha=\text{O}$) syringyl units (S')
G_2	111.7/6.97	$\text{C}_2\text{-H}_2$ in guaiacyl units (G)
G_5	115.4/6.69 and 115.9/6.78	$\text{C}_5\text{-H}_5$ in guaiacyl units (G)
G_6	119.9/6.79	$\text{C}_6\text{-H}_6$ in guaiacyl units (G)
$\text{PB}_{2,6}$	131.5/7.67	$\text{C}_{2,6}\text{-H}_{2,6}$ in <i>p</i> -hydroxybenzoate substructures (PB)

Table S2 Assignment of the association carbohydrate ^{13}C - ^1H cross-signals in the HSQC spectra

label	$\delta\text{C}/\delta\text{H}$	assignment
X_2	70.6/3.03	$\text{C}_2\text{-H}_2$ in $\beta\text{-D-xylopyranoside}$
X_3	74.2/3.24	$\text{C}_3\text{-H}_3$ in $\beta\text{-D-xylopyranoside}$
X_4	75.0/3.74	$\text{C}_4\text{-H}_4$ in $\beta\text{-D-xylopyranoside}$
X_{3_1}	101.4/4.20	3- <i>O</i> -acetyl- $\beta\text{-D-xylopyranoside}$

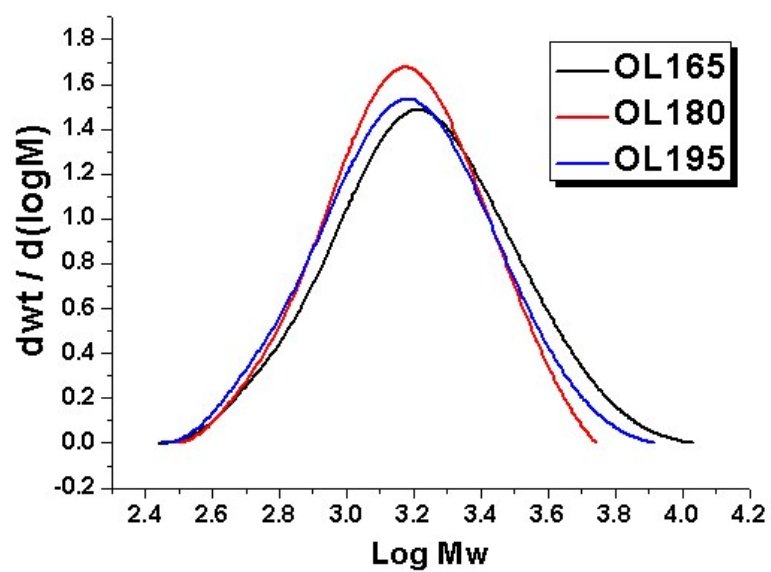


Figure S1 GPC curves of the lignin fractions.

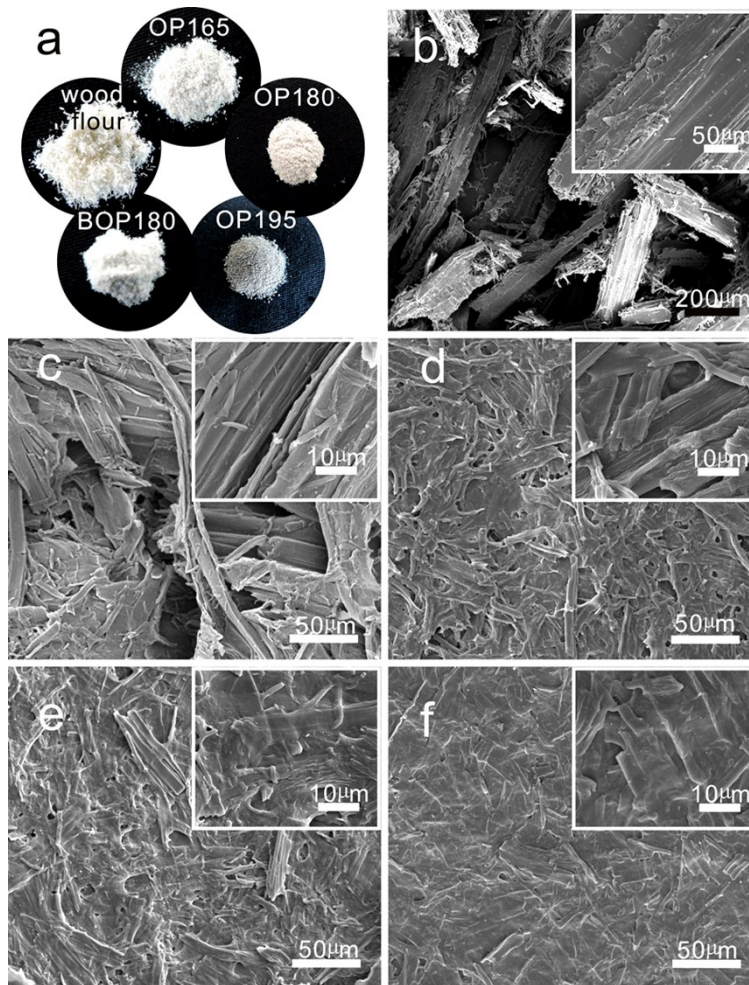


Figure S2 (a) Photographs of raw wood feedstock and the pretreated samples. SEM images of (b) wood flour, (c) OP165, (d) OP180, (e) OP195 and (f) BOP180.

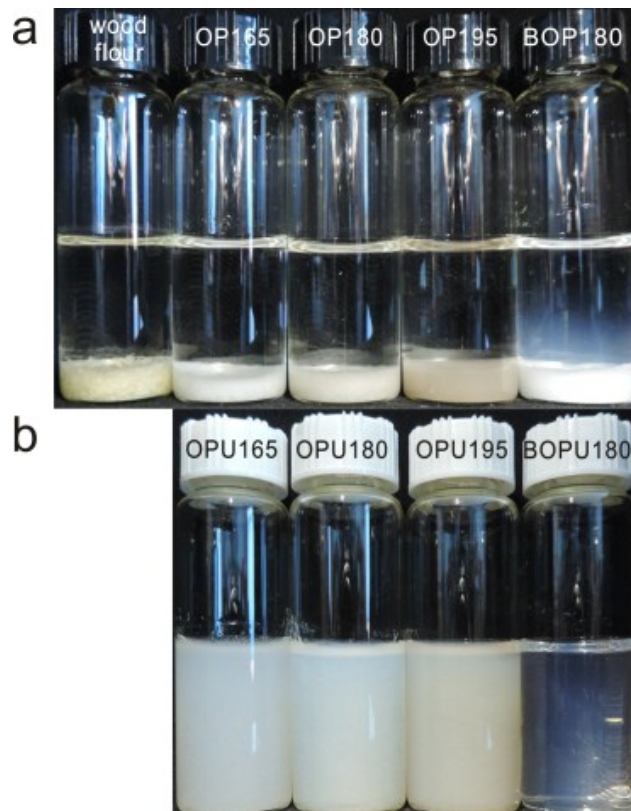


Figure S3 Sedimentation observation of (a) wood flour and the pretreated samples, and (b) the CNC suspensions. The photograph was taken after the samples had been placed for six months.

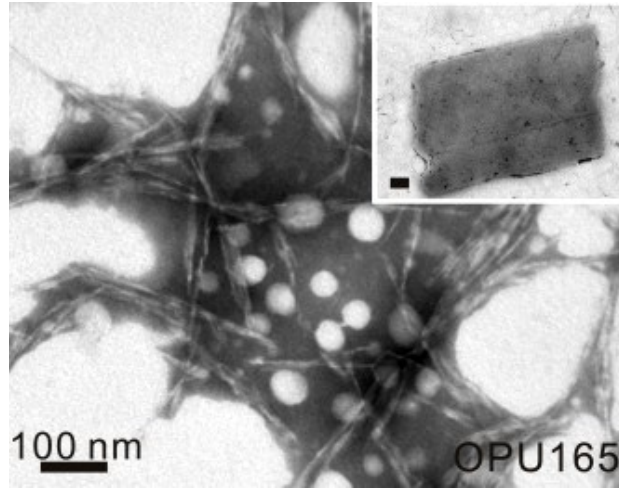


Figure S4 TEM image of OPU165 CNCs, and the inset shows the non-disintegrated cytoderm fragment.

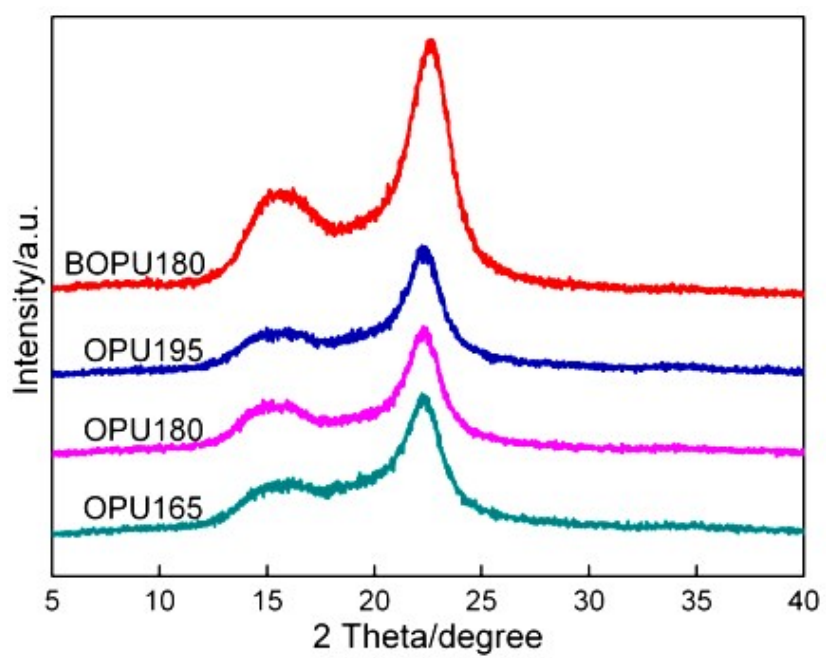


Figure S5 XRD patterns of OPU samples and BOPU180

CNC-based aerogels were obtained by freeze-drying the CNC suspensions. The SEM images in Fig. S6 demonstrate that the aerogels were composed of massive membranes, which were formed through the mutual aggregation of CNCs. Micrometer-sized pores were enclosed by the membranes, whereas mesopores could be identified on the membrane surfaces.

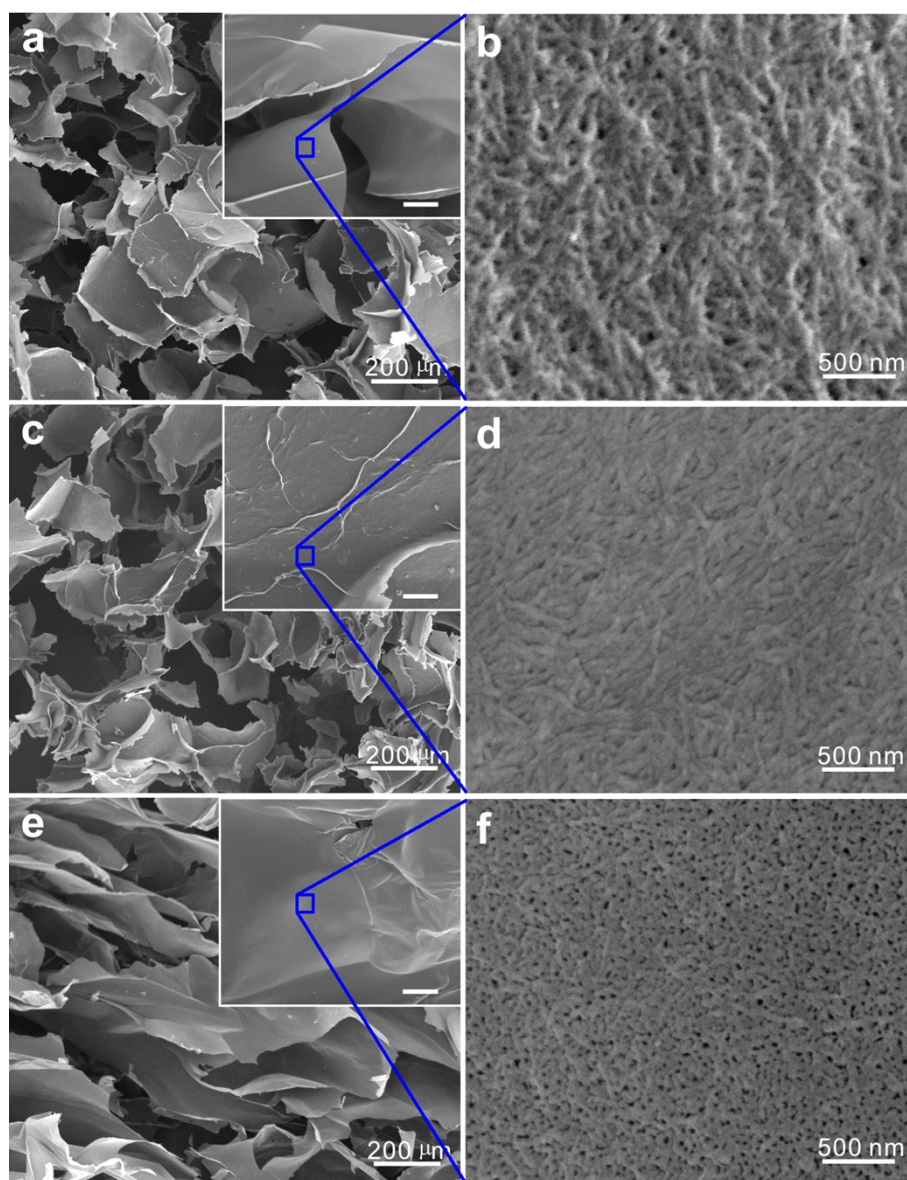


Figure S6 SEM images of the aerogels constituted by: (a-b) OPU180, (c-d) OPU195, and (e-f) BOPU180 CNCs. The scale bar in the insets corresponds to 20 μm .